

See discussions, stats, and author profiles for this publication at: <https://www.researchgate.net/publication/320927057>

Structural and electronic properties of $\text{Cu}_x\text{Ag}_{1-x}\text{Cl}$: First-principles study

Article in *European Physical Journal Plus* · November 2017

DOI: 10.1140/epjp/i2017-11733-0

CITATIONS

3

READS

266

5 authors, including:



Hamza Rekab Djabri

Ecole Nationale Polytechnique d'Oran

20 PUBLICATIONS 8 CITATIONS

[SEE PROFILE](#)



Souad Louhibi-Fasla

ENP d'ORAN

24 PUBLICATIONS 69 CITATIONS

[SEE PROFILE](#)



S. Amari

Hassiba Benbouali University of Chlef

42 PUBLICATIONS 178 CITATIONS

[SEE PROFILE](#)



Bahlouli Soumia

Université des Sciences et de la Technologie d'Oran Mohamed Boudiaf

14 PUBLICATIONS 17 CITATIONS

[SEE PROFILE](#)

Some of the authors of this publication are also working on these related projects:



Prediction and simulation of nanomaterial properties for optoelectronic applications [View project](#)



alloys [View project](#)

Eur. Phys. J. Plus (2017) **132**: 471

DOI 10.1140/epjp/i2017-11733-0

Structural and electronic properties of $\text{Cu}_x\text{Ag}_{1-x}\text{Cl}$: First-principles study

H. Rekab-Djabri, S. Louhibi-Fasla, S. Amari, S. Bahlouli and M. Elchikh



Structural and electronic properties of $\text{Cu}_x\text{Ag}_{1-x}\text{Cl}$: First-principles study

H. Rekab-Djabri^{1,2}, S. Louhibi-Fasla^{1,a}, S. Amari³, S. Bahlouli⁴, and M. Elchikh⁴

¹ Laboratoire de Micro et de Nanophysique LaMiN – ENP d'ORAN, BP 1523, El M'Naouer, 31000, Algeria

² Faculté de SNVST, Université AKLI Mohand-Oulhadj, Bouira, Algeria

³ Laboratoire de Modélisation et de Simulation en Sciences des Matériaux, Université Djillali Liabès, Sidi Bel-Abbes, Algeria

⁴ LPMF USTO-MB BP 1505 Oran El M'Naouer, Oran, 31000, Algeria

Received: 22 March 2016 / Revised: 7 July 2017

Published online: 9 November 2017 – © Società Italiana di Fisica / Springer-Verlag 2017

Abstract. The structural and electronic properties of the ternary $\text{Cu}_x\text{Ag}_{1-x}\text{Cl}$ alloy are investigated using a recent version of the full potential linear muffin-tin orbitals method (FPLMTO) based on the density functional theory, within both the local density approximation (LDA) and the generalized gradient approximation (GGA). The lattice constants, bulk modulus and band gap were calculated as a function of copper molar fraction x in rock salt ($B1$) and zincblende ($B3$) structures. These parameters were found to depend non-linearly on alloy concentration Cu, except for the lattice parameter which follows Vegard's law. Our results predict the rock salt phase as the ground state for this ternary system.

1 Introduction

In recent years, there is a continuous interest in the study of the structural and electronic properties of silver halides such as AgCl, due to their importance in the photographic processes [1], as well as in photo and electro-chemistry [2]. The copper halides, especially CuCl, are prototype materials for non-linear optical experiments [3], and present many unusual features compared with the III–V and II–VI compounds [4]. Recently Ameri [5, 6] investigated the structural and electronic properties of $\text{CuCl}_{1-x}\text{I}_x$ and $\text{Cu}_x\text{Ag}_{1-x}\text{I}$ ternary alloys. Another theoretical study [7] investigated the structural, electronic and thermodynamic properties of ordered $\text{Cu}_x\text{Ag}_{1-x}\text{I}$. On the other hand, we previously published the results of a study of both bulk and superlattice systems of copper halides within the ab initio method [8]. Despite the technological importance of AgCl and CuCl binary compounds the CuAgCl alloy system has never been explored to the best of our knowledge. Keeping in view that the lattice mismatch between CuCl and AgCl is very small we extend our work in the present paper to $\text{Cu}_x\text{Ag}_{1-x}\text{Cl}$ alloys. The experiments have shown that the atomic ground states of AgCl correspond to the rock salt ($B1$) structure (space group Fm-3m), a form that they have in common with the majority of the alkali halides. On the other hand, CuCl and other I–VII semiconducting copper halides are known to be semiconductors with large and direct gaps in their zincblende ($B3$) ground state phase (space group F43m). Our aim is to get further insight into the nature of the CuAgCl alloy in the $B1$ and $B3$ phases. Otherwise the objective of this work is to predict the ground state properties and the nature of the band structure for this ternary alloy *versus* copper concentration. The knowledge of physical properties of this alloy provides an insight view about its performance in practical applications.

So, we have investigated the structural and electronic properties of $\text{Cu}_x\text{Ag}_{1-x}\text{Cl}$ (hereafter, $0 \leq x \leq 1$ denotes the molar fraction of Cu), by performing ab initio calculations based on the full-potential linear muffin-tin orbital within the density functional theory. This paper is organized as follows: A brief description of the computational details and methodology is given in sect. 2. We present the theoretical results and discussion concerning the structural and electronic properties in sect. 3 and the conclusion is given in sect. 4.

^a e-mail: fasbenplast@yahoo.fr (corresponding author)

Table 1. The plane wave number (NPW), energy cut-off (E_{cut}) (in Ry) and the muffin-tin spheres radius (RMTS) (in u.a.) used in the calculation for binary CuCl and AgCl compounds and for their corresponding alloys in $B3$ and $B1$ structures.

| Structure | Compound | NPW | | E_{cut} (Ry) | | RMTS (u.a) | | | | | |
|-----------|---|------|------|-----------------------|-------|------------|-------|-------|-------|-------|-------|
| | | LDA | GGA | LDA | GGA | Cu | | Ag | | Cl | |
| | | | | | | LDA | GGA | LDA | GGA | LDA | GGA |
| $B3$ | AgCl | 895 | 148 | 45.12 | 52.7 | 2.322 | 2.150 | 2.220 | 2.154 | 2.420 | 2.154 |
| | $\text{Cu}_{0.25}\text{Ag}_{0.75}\text{Cl}$ | 562 | 1542 | 65.0 | 52.1 | 2.152 | 2.165 | 2.250 | 2.450 | 2.523 | 2.145 |
| | $\text{Cu}_{0.5}\text{Ag}_{0.5}\text{Cl}$ | 452 | 875 | 32.57 | 42.0 | 2.152 | 2.135 | 2.154 | 2.145 | 2.845 | 2.425 |
| | $\text{Cu}_{0.75}\text{Ag}_{0.25}\text{Cl}$ | 1452 | 1607 | 44.157 | 87.12 | 2.452 | 2.152 | 2.125 | 2.455 | 2.154 | 2.120 |
| $B1$ | CuCl | 1850 | 2010 | 17.8 | 45.40 | 2.548 | 2.154 | 2.985 | 2.542 | 2.710 | 2.253 |
| | AgCl | 875 | 2006 | 52.4 | 20.6 | 2.080 | 2.452 | 2.125 | 2.647 | 2.10 | 2.755 |
| | $\text{Cu}_{0.25}\text{Ag}_{0.75}\text{Cl}$ | 642 | 690 | 53.22 | 10.9 | 2.520 | 2.591 | 2.333 | 2.599 | 2.54 | 2.52 |
| | $\text{Cu}_{0.5}\text{Ag}_{0.5}\text{Cl}$ | 652 | 690 | 65.17 | 10.9 | 2.455 | 2.591 | 2.455 | 2.591 | 2.455 | 2.54 |
| | $\text{Cu}_{0.75}\text{Ag}_{0.25}\text{Cl}$ | 1470 | 2745 | 56.25 | 100.2 | 2.652 | 2.632 | 2.458 | 2.132 | 2.758 | 2.13 |
| | CuCl | 2450 | 1045 | 45.28 | 42 | 2.520 | 2.754 | 2.451 | 2.244 | 2.154 | 2.145 |

2 Computational details

In this study, the first-principles calculations are performed using the FPLMTO method [9, 10] augmented by a plane-wave basis (PLW) based on the density functional theory (DFT), as implemented in the Lmtart code [11]. The exchange and correlation potential was calculated using the local density approximation (LDA) [12] and the generalized approximation (GGA) [13]. This is an improved method compared to the previous ones which treats muffin-tin spheres and interstitial regions on the same footing, leading to improvements in the precision of the eigenvalues. At the same time, this method in which the space is divided into an interstitial regions and non-overlapping muffin-tin spheres (MTS) surrounding the atomic sites, uses a more complete basis than its predecessors. In the interstitial regions, the basis functions are represented by the Fourier series. Inside the MTS, the basis functions are represented in terms of numerical solutions of the radial Schrödinger equation for the spherical part of the potential multiplied by spherical harmonics. The charge density and the potential are represented inside the MTS by spherical harmonics up to $l_{\text{max}} = 6$. The self-consistent calculations are considered to be converged when the total energy of the system is stable within 10^{-5} Ry. In order to avoid the overlap of atomic spheres, the muffin-tin spheres radius for each atomic position is taken to be different for each case. Both the plane waves cut-off are varied to ensure the total energy convergence. The values of the muffin-tin spheres radius (RMTS), number of plane waves (NPW), used in our calculation are summarized in table 1.

3 Results and discussion

3.1 Structural properties

In this section the structural properties of the binary compounds CuCl, AgCl and their ternary alloys $\text{Cu}_x\text{Ag}_{1-x}\text{Cl}$ were analyzed in the zincblende ($B3$) and rock salt ($B1$) structures. The alloys were modeled at some selected compositions $x = 0.25, 0.5, 0.75$ with ordered structures described in terms of periodically repeated supercells. For the considered structures, we perform the structural optimization by minimizing the total energy with respect to the cell parameters and also to the atomic positions presented in table 2. The obtained results for $\text{Cu}_x\text{Ag}_{1-x}\text{Cl}$ with ($x = 0, 0.25, 0.5, 0.75$ and 1), in $B1$ and $B3$ phases are shown in fig. 1 using GGA and LDA approximations.

It is seen from this figure that the ground state in $\text{Cu}_x\text{Ag}_{1-x}\text{Cl}$ is that of the $B1$ phase for $x = 0, 0.25, 0.5$ and 0.75 at ambient conditions, but for $x = 1$ the binary is stable in $B3$ phase. The structural properties of $\text{Cu}_x\text{Ag}_{1-x}\text{Cl}$ alloys are calculated by energy minimization process. In this process, the unit cell volume is varied and the corresponding unit cell energy is evaluated. The unit cell energy *versus* the volume is fitted by the Murnaghan equation of state [14].

Table 2. Atomic positions for $\text{Cu}_x\text{Ag}_{1-x}\text{Cl}$ alloys.

| Phase | X | Atom | Atomic position |
|-----------|------|--|--|
| <i>B3</i> | 0.0 | Cl | $(1/4 \ 1/4 \ 1/4), (3/4 \ 3/4 \ 1/4), (3/4 \ 1/4 \ 3/4), (1/4 \ 3/4 \ 3/4)$ |
| | | Ag | $(0 \ 1/2 \ 1/2), (1/2 \ 0 \ 1/2), (1/2 \ 1/2 \ 0), (0 \ 0 \ 0)$ |
| | 0.25 | Cl | $(1/4 \ 1/4 \ 1/4), (3/4 \ 3/4 \ 1/4), (3/4 \ 1/4 \ 3/4), (1/4 \ 3/4 \ 3/4)$ |
| | | Ag | $(0 \ 1/2 \ 1/2), (1/2 \ 0 \ 1/2), (1/2 \ 1/2 \ 0)$ |
| | | Cu | $(0 \ 0 \ 0)$ |
| | 0.5 | Cl | $(1/4 \ 1/4 \ 1/4), (3/4 \ 3/4 \ 1/4), (3/4 \ 1/4 \ 3/4), (1/4 \ 3/4 \ 3/4)$ |
| | | Ag | $(0 \ 1/2 \ 1/2), (1/2 \ 0 \ 1/2)$ |
| | | Cu | $(0 \ 0 \ 0), (1/2 \ 1/2 \ 0)$ |
| | 0.75 | Cl | $(1/4 \ 1/4 \ 1/4), (3/4 \ 3/4 \ 1/4), (3/4 \ 1/4 \ 3/4), (1/4 \ 3/4 \ 3/4)$ |
| | | Ag | $(0 \ 1/2 \ 1/2)$ |
| | | Cu | $(0 \ 0 \ 0), (1/2 \ 0 \ 1/2), (1/2 \ 1/2 \ 0)$ |
| | 1.0 | Cl | $(1/4 \ 1/4 \ 1/4), (3/4 \ 3/4 \ 1/4), (3/4 \ 1/4 \ 3/4), (1/4 \ 3/4 \ 3/4)$ |
| Cu | | $(0 \ 1/2 \ 1/2), (1/2 \ 0 \ 1/2), (1/2 \ 1/2 \ 0), (0 \ 0 \ 0)$ | |
| <i>B1</i> | 0.0 | Cl | $(1/4 \ 1/4 \ 1/4), (3/4 \ 3/4 \ 1/4), (3/4 \ 1/4 \ 3/4), (1/4 \ 3/4 \ 3/4)$ |
| | | Ag | $(0 \ 1/2 \ 1/2), (1/2 \ 0 \ 1/2), (1/2 \ 1/2 \ 0), (0 \ 0 \ 0)$ |
| | 0.25 | Cl | $(1/2 \ 1/2 \ 1/2), (1.0 \ 1.0 \ 1/2), (1.0 \ 1/2 \ 1.0), (1/2 \ 1.0 \ 1.0)$ |
| | | Ag | $(0 \ 1/2 \ 1/2), (1/2 \ 0 \ 1/2), (1/2 \ 1/2 \ 0)$ |
| | | Cu | $(0 \ 0 \ 0)$ |
| | 0.5 | Cl | $(1/2 \ 1/2 \ 1/2), (1.0 \ 1.0 \ 1/2), (1.0 \ 1/2 \ 1.0), (1/2 \ 1.0 \ 1.0)$ |
| | | Ag | $(0 \ 1/2 \ 1/2), (1/2 \ 0 \ 1/2)$ |
| | | Cu | $(0 \ 0 \ 0), (1/2 \ 1/2 \ 0)$ |
| | 0.75 | Cl | $(1/2 \ 1/2 \ 1/2), (1.0 \ 1.0 \ 1/2), (1.0 \ 1/2 \ 1.0), (1/2 \ 1.0 \ 1.0)$ |
| | | Ag | $(0 \ 1/2 \ 1/2)$ |
| | | Cu | $(0 \ 0 \ 0), (1/2 \ 1/2 \ 0), (1/2 \ 0 \ 1/2)$ |
| | 1.0 | Cl | $(1/4 \ 1/4 \ 1/4), (3/4 \ 3/4 \ 1/4), (3/4 \ 1/4 \ 3/4), (1/4 \ 3/4 \ 3/4)$ |
| Cu | | $(0 \ 1/2 \ 1/2), (1/2 \ 0 \ 1/2), (1/2 \ 1/2 \ 0), (0 \ 0 \ 0)$ | |

All the ground state properties for each composition such as the equilibrium lattice constant a_0 , the bulk modulus B_0 , the bulk modulus pressure derivative B' in *B1* and *B3* phases using both the LDA and GGA are presented in table 3 and compared with the available experimental and other theoretical data. The lattice constants obtained within the GGA for the parent binary system AgCl (in *B1* structure) and CuCl (in *B3* structure) are, respectively, 2.93% and 1.41% lower than the experimental value [15, 16], which is the usual level of accuracy of the GGA. When comparing the results obtained within the LDA, the lattice constants are 3.11% for AgCl (in *B1*) and 2.91% for CuCl (in *B3*) and are larger than the experimental values [15, 16]. Our results regarding B_0 for *B1* and *B3* phases of CuCl and AgCl binary are in reasonable agreement with the literature [16, 17]. To the best of our knowledge, there are no data available in the literature for Cu concentrations of 25%, 50%, and 75%. On the other hand, the B_0 calculated for CuCl in the *B1* and *B3* structures are larger than those of AgCl for both LDA and GGA approximations.

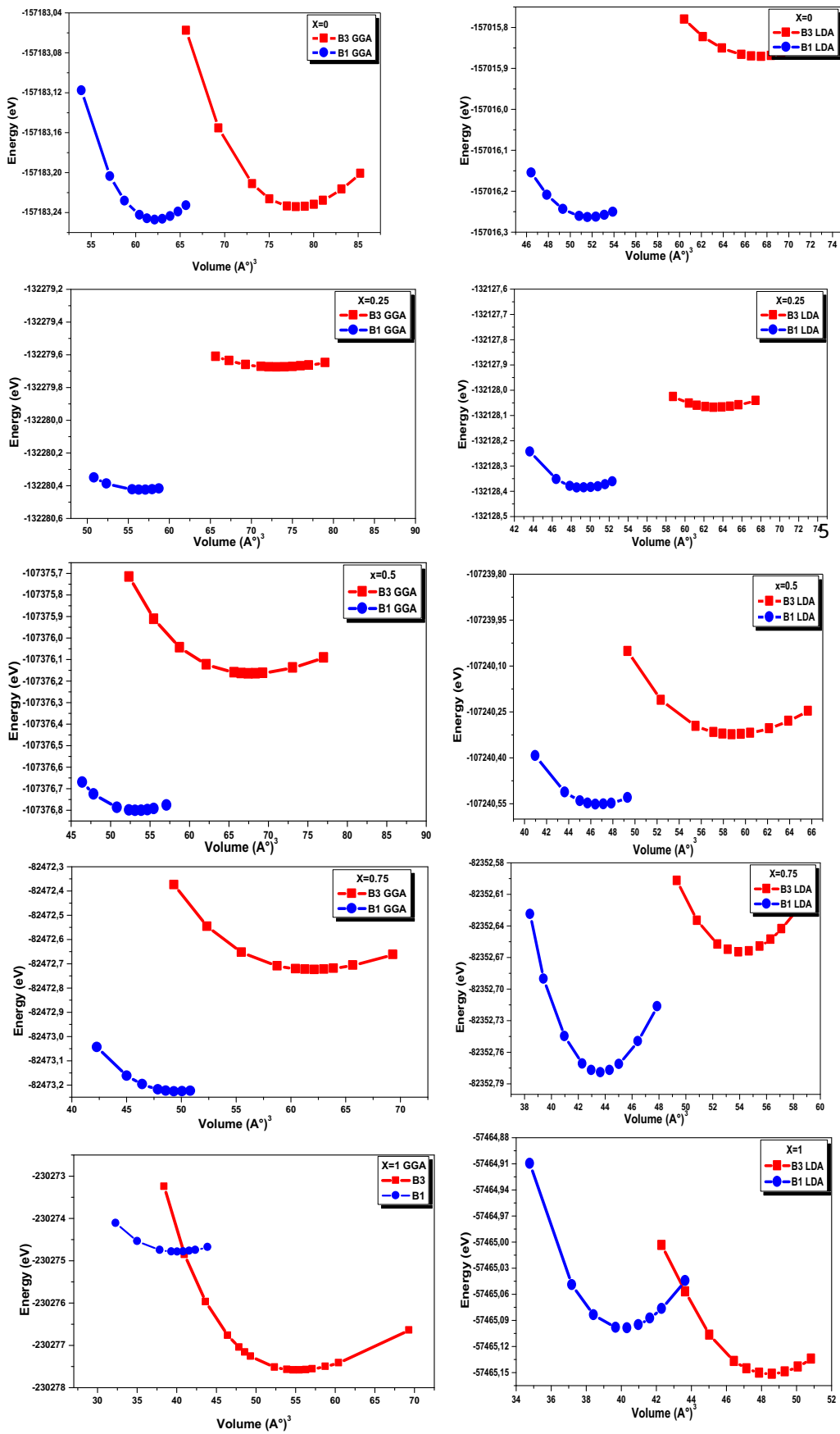


Fig. 1. Variation of total energies *versus* the volume of unit cell for B1 and B3 structures of $\text{Cu}_x\text{Ag}_{1-x}\text{Cl}$ ($x = 0, 0.25, 0.5, 0.75, \text{ and } 1$), with LDA and GGA approximations.

Table 3. Calculated lattice parameter a , bulk modulus B_0 and the bulk modulus pressure derivative B' compared to experimental and other theoretical values of CuCl and AgCl and their alloys, in $B1$ and $B3$ phases using both the LDA and GGA.

| Phase | | Material | | a_{eq} (Å) | | B_0 (GPa) | | B'_0 | | |
|---------------------------------------|------|---|------------|----------------------|-----------------------|----------------------|-----------------------|----------------------|----------------------|---------------------|
| $\text{Cu}_x\text{Ag}_{1-x}\text{Cl}$ | x | | | GGA | LDA | GGA | LDA | GGA | LDA | |
| $B3$ | 0 | AgCl | This work | 6.166 | 5.866 | 44.573 | 74.58 | 4.978 | 5.109 | |
| | | | Other work | 6.08 ^(d) | 5.78 ^(d) | 30.13 ^(d) | 49.33 ^(d) | | | |
| | | | Expr | | | | | | | |
| | 0.25 | $\text{Cu}_{0.25}\text{Ag}_{0.75}\text{Cl}$ | | 6.032 | 5.748 | 49.133 | 80.32 | 5.077 | 5.157 | |
| | | | | | | | | | | |
| | 0.5 | $\text{Cu}_{0.5}\text{Ag}_{0.5}\text{Cl}$ | | 5.882 | 5.611 | 53.400 | 86.49 | 4.905 | 5.155 | |
| | 0.75 | $\text{Cu}_{0.75}\text{Ag}_{0.25}\text{Cl}$ | | 5.705 | 5.452 | 60.755 | 99.15 | 5.067 | 5.102 | |
| | 1 | CuCl | This work | 5.498 | 5.262 | 72.671 | 131.2 | 4.125 | 4.74 | |
| | | | Other work | 5.455 ^(b) | 5.2578 ^(a) | 48.38 ^(b) | 68.993 ^(a) | 5.196 ^(b) | 5.075 ^(a) | |
| | | | Expr | 5.42 ^(e) | | 39.8 ^(f) | | 4 ^(e) | | |
| | $B1$ | 0 | AgCl | This work | 5.716 | 5.375 | 61.93 | 115.03 | 4.190 | 4.923 |
| | | | | Other work | 5.617 ^(c) | 5.368 ^(c) | 43.318 ^(c) | 71.61 ^(c) | 4.40 ^(c) | 5.21 ^(c) |
| Expr | | | | 5.548 ^(g) | | 47 ^(h) | | 4 ^(h) | | |
| 0.25 | | $\text{Cu}_{0.25}\text{Ag}_{0.75}\text{Cl}$ | | 5.629 | 5.292 | 65.46 | 117.09 | 4.545 | 5.383 | |
| | | | | | | | | | | |
| 0.5 | | $\text{Cu}_{0.5}\text{Ag}_{0.5}\text{Cl}$ | | 5.528 | 5.195 | 65.90 | 122.09 | 5.222 | 5.171 | |
| 0.75 | | $\text{Cu}_{0.75}\text{Ag}_{0.25}\text{Cl}$ | | 5.303 | 5.077 | 87.97 | 130.9 | 4.503 | 5.077 | |
| 1 | | CuCl | This work | 5.313 | 4.936 | 74.58 | 146.07 | 4.190 | 4.936 | |
| | | | Other work | 5.156 ^(b) | 4.935 ^(a) | 59.05 ^(b) | 94.148 ^(a) | 4.733 ^(b) | 4.905 ^(a) | |
| | | | Expr | 4.929 ^(e) | | | | 4 ^(e) | | |

^(a) Ref. [8].^(b) Ref. [18].^(c) Ref. [19].^(d) Ref. [20].^(e) Ref. [21].^(f) Ref. [22].^(g) Ref. [15].^(h) Ref. [23].

On the whole, our calculated structural parameters are in good agreement with those obtained by first-principles methods within different approximations. Usually, in the treatment of alloys when the experimental data are scarce, it is assumed that the atoms are located at the ideal lattice sites and the lattice constant varies linearly with composition x according to the so-called Vegard's law [24]:

$$a(A_xB_{1-x}C) = xa_{AC} + (1-x)a_{BC},$$

where a_{AC} and a_{BC} are the equilibrium lattice constants of the binary compounds AC and BC, respectively, and $(A_xB_{1-x}C)$ is the alloy lattice constant.

In fig. 2, we present the calculated lattice constants for $\text{Cu}_x\text{Ag}_{1-x}\text{Cl}$ versus concentration x along with Vegard's law result. The lattice constant scales linearly with composition x thus obeying Vegard's law. Our calculations exhibit an excellent agreement to Vegard's law for the rock salt structure and a small deviation for the zinblende structure. The overall behaviors of the variation of bulk modulus as a function of the composition x is presented in fig. 3. We remark a significant deviation from the linear concentration using the LDA approximation. So, the use of the GGA in this work is more appropriate than the LDA and correctly predicts the composition dependence x of the calculated bulk modulus. A small deviation of the bulk modulus from the linear concentration dependence with the GGA is observed and should be mainly due to the bulk modulus mismatch between AgCl and CuCl compounds.

A more precise comparison for the behavior of $\text{Cu}_x\text{Ag}_{1-x}\text{Cl}$ ternary alloys with the GGA approximation shows that a decrease of the lattice constant is accompanied by an increase of the bulk modulus. It represents bond strengthening or weakening effects induced by changing the composition. Figure 4 shows a linear variation of the difference of energy local minimum of $B1$, $B3$, versus composition x . It is clearly seen that the ternary alloy $\text{Cu}_x\text{Ag}_{1-x}\text{Cl}$ changes from $B1$ to $B3$ phases when x is larger or equal to 0.920 and 0.975 with the LDA and GGA, respectively.

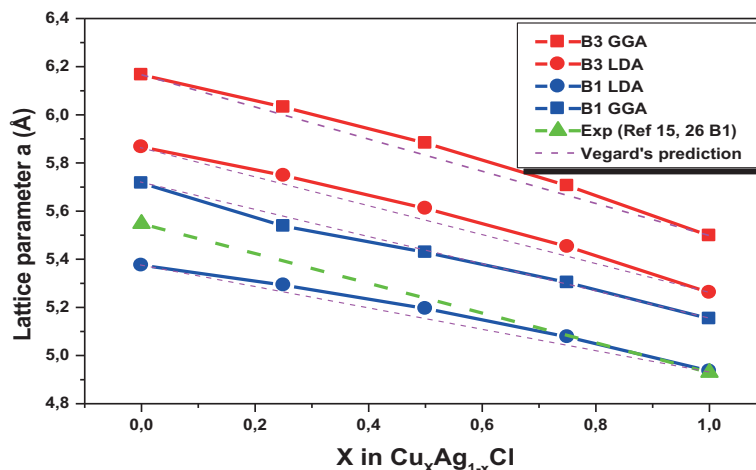


Fig. 2. Composition dependence of the calculated lattice constants (solid squares and circles) of $\text{Cu}_x\text{Ag}_{1-x}\text{Cl}$ alloy compared with Vegard's prediction (magenta dashed line) and Exp (ref. [15,16] B1) (green dashed line).

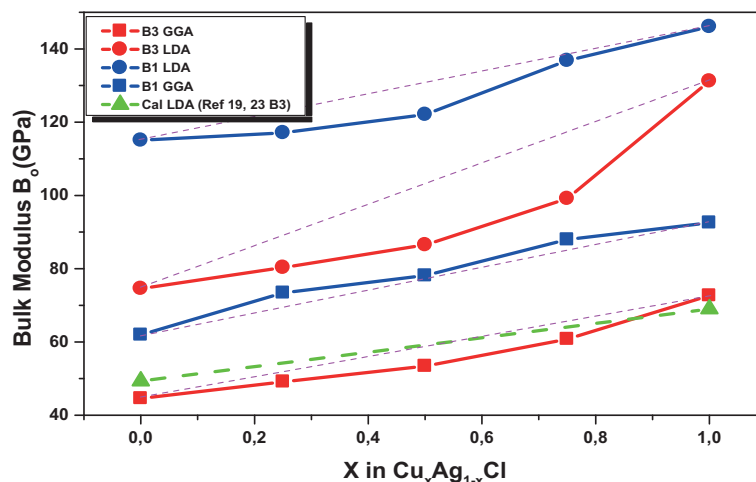


Fig. 3. Composition dependence of the calculated bulk modulus (solid squares) of $\text{Cu}_x\text{Ag}_{1-x}\text{Cl}$ alloy compared with the linear composition dependence prediction (magenta dashed line), and Cal (ref. [8] and [20] B3), (green dashed line).

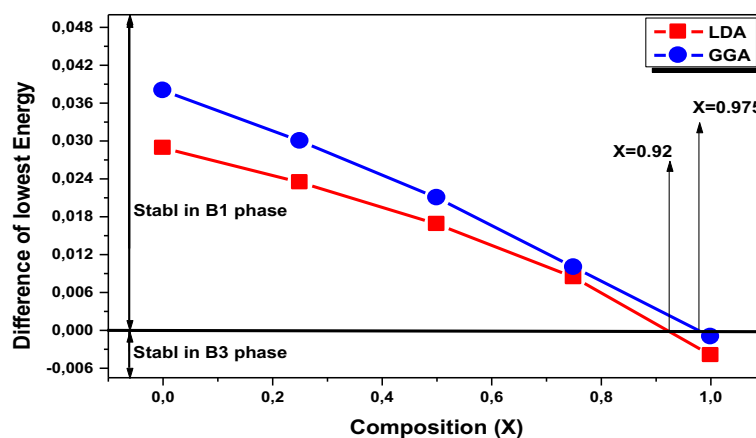


Fig. 4. Composition dependence of energy ground state of $\text{Cu}_x\text{Ag}_{1-x}\text{Cl}$ ($x = 0, 0.25, 0.5, 0.75, 1$) in B1 and B3.

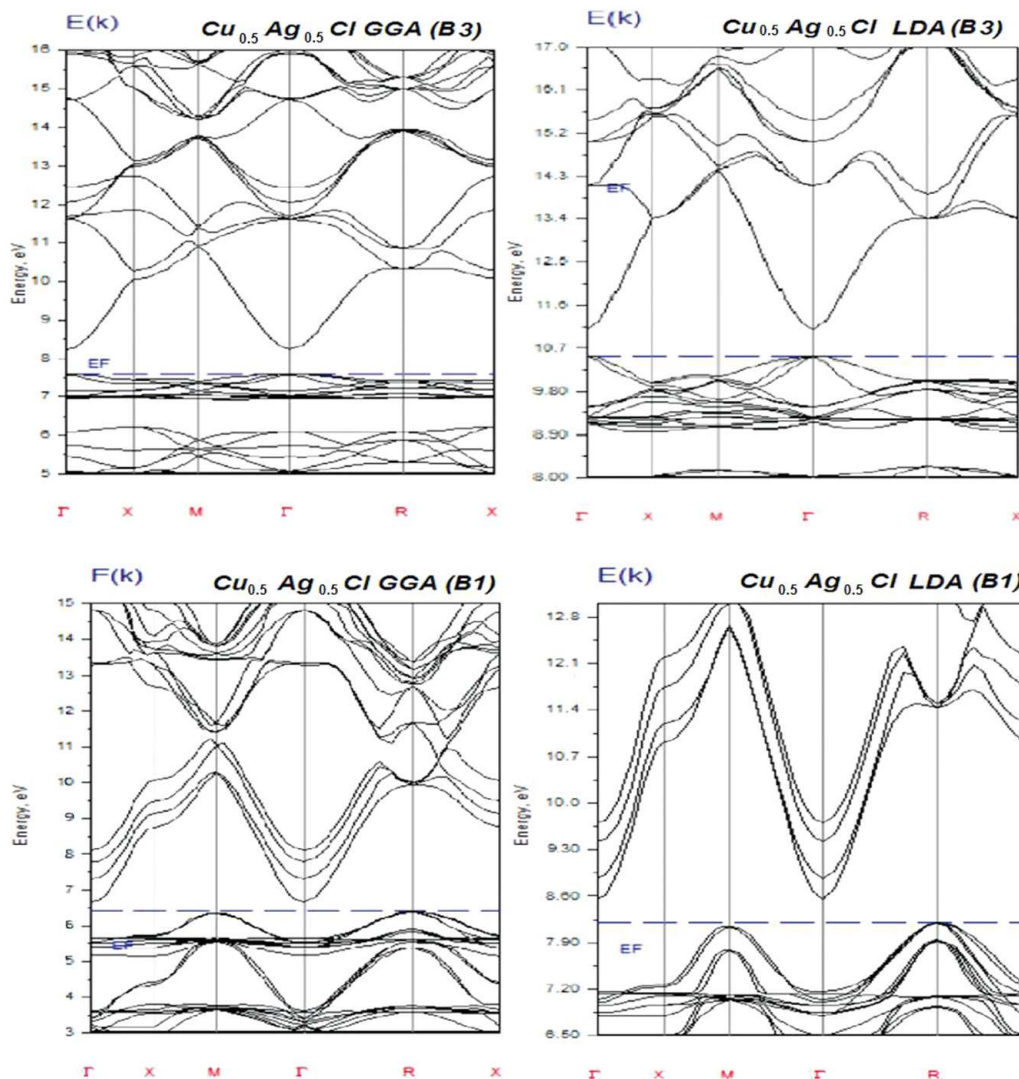


Fig. 5. The band structure of B1- $\text{Cu}_{0.5}\text{Ag}_{0.5}\text{Cl}$ and B3- $\text{Cu}_{0.5}\text{Ag}_{0.5}\text{Cl}$ with LDA and GGA approximations.

3.2 Electronic properties

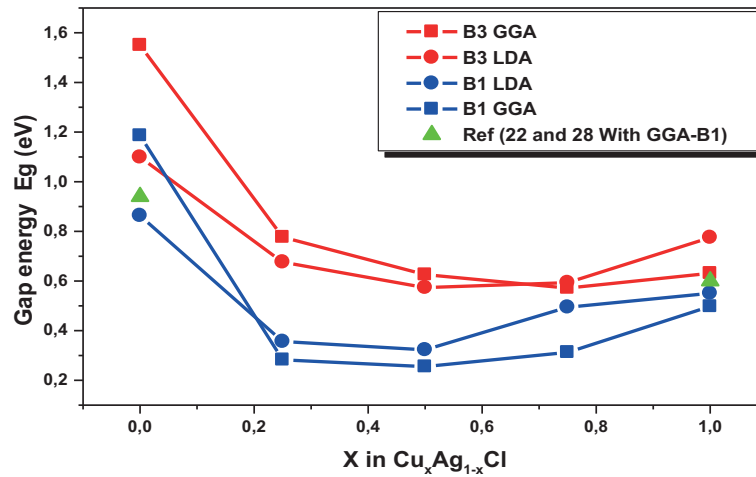
Based on the optimized structural results, the electronic band structures corresponding to high symmetry points are obtained within the GGA and LDA for the B3 and B1 structures. A Fermi level (EF) is chosen to locate at 0 eV and coincides with the top of the valence band. Figure 5 shows the band structure of $\text{Cu}_x\text{Ag}_{1-x}\text{Cl}$ at $x = 0.5$ in the rock salt and zincblende structures, respectively. The values of the energy band gap for each structure of $\text{Cu}_x\text{Ag}_{1-x}\text{Cl}$ ternary alloys versus Cu concentration are presented in table 4 and plotted in fig. 6. Our results of band gap for the binary compounds are in good agreement with the experiment and the theoretical works. The band gap for B1-AgCl-GGA is 1.086 eV, which is in good agreement with Benmessabih *et al.* results (0.94 eV with the GGA) [19], and the band gap for B3-CuCl-LDA is 0.775 eV, which is in very good agreement with Badi *et al.* results (0.756 eV with the LDA) [8]. For the other concentrations of alloys, there are no results for comparing our band structure.

It can be seen from table 4 that the gap decreases with the increase of Cu concentrations up to 0.5 in the rock salt and zincblende phase with the LDA and GGA respectively. When x is more than 0.5 the gap increases with the increase of Cu. The variation of this gap is nonlinear and the band gap is the largest one at $x = 1$.

Table 4. Calculated band gap energy of $\text{Cu}_x\text{Ag}_{1-x}\text{Cl}$ alloys at different Cu concentrations (all values are in eV).

| X | Present work | | | | | | Other work | | |
|------|-------------------------|--------|---------------------|----------|----------|----------------------|----------------------|---------------------|--|
| | Value of Gap E_g (eV) | | Nature of Gap | | | LDA | GGA | Expr | |
| | LDA | GGA | LDA | GGA | | | | | |
| 0 | 0.8633 | 1.086 | M- Γ | Indirect | Indirect | 0.636 ^(c) | 0.94 ^(c) | 3.2 ^(e) | |
| 0.25 | 0.3564 | 0.2822 | M- Γ | Indirect | Indirect | | | | |
| $B1$ | 0.5 | 0.3225 | M- Γ | Indirect | Indirect | | | | |
| 0.75 | 0.4947 | 0.3125 | M- Γ | Indirect | Indirect | | | | |
| 1 | 0.5503 | 0.4973 | M- Γ | Indirect | Indirect | 0.6 ^(f) | | | |
| 0 | 1.0987 | 1.5501 | Γ - Γ | Direct | Direct | | | | |
| 0.25 | 0.6761 | 0.7769 | Γ - Γ | Direct | Direct | | | | |
| $B3$ | 0.5 | 0.5734 | Γ - Γ | Direct | Direct | | | | |
| 0.75 | 0.5934 | 0.5716 | Γ - Γ | Direct | Direct | | | | |
| 1 | 0.7752 | 0.6311 | Γ - Γ | Direct | Direct | 0.756 ^(a) | 0.509 ^(b) | 3.40 ^(d) | |

- (a) Ref. [8].
(b) Ref. [25].
(c) Ref. [19].
(d) Ref. [26].
(e) Ref. [27].
(f) Ref. [28].

**Fig. 6.** Concentration dependence of the band gaps calculated by different exchange-correlation energy approximations for $\text{Cu}_x\text{Ag}_{1-x}\text{Cl}$ alloy. The measured value is taken from refs. [19, 28].

As a result of the drawn band structures with LDA and GGA approximations, we found that $\text{Cu}_{0.5}\text{Ag}_{0.5}\text{Cl}$ ternary alloy compounds have an indirect gap at M- Γ for the rock salt phase with an energy of 0.3225 and 0.2552 eV, respectively, for the LDA and GGA and a direct gap at the Γ point for the zincblende phase with an energy of 0.5734 and 0.6259 eV, respectively for the LDA and GGA. We have found that the $\text{Cu}_x\text{Ag}_{1-x}\text{Cl}$ local minimum changes from $B1$ to $B3$ when x is larger or equal to 0.920 and 0.975 with both the LDA and GGA, respectively. These values are so very close to $x = 1$. Indeed we can see in fig. 4 that in most phases in the diagram the system is in the rock salt phase. So these results predict the $B1$ phase as the ground state for this ternary system.

4 Conclusion

In this work, we have performed first-principles total energy calculations to predict the ground state properties and the nature of the band structure for new ordered $\text{Cu}_x\text{Ag}_{1-x}\text{Cl}$ ternary alloys *versus* copper concentration. Studies were carried out using a recent version of the full potential linear muffin-tin orbitals method (FPLMTO) within the local density approximation (LDA) and the generalized approximation (GGA). We have studied the variation of the lattice constants, bulk modulus and band energy as a function of the alloy concentration in the rock salt (*B1*) and zincblende (*B3*) phases. Our results show that the use of the GGA is more appropriate than the LDA and correctly predicts the composition dependence x of the bulk modulus. The lattice parameters of the $\text{Cu}_x\text{Ag}_{1-x}\text{Cl}$ compounds scale linearly with Cu concentration and the results exhibit small deviation from Vegard's behavior for zincblende structure. The electronic band structure shows a nonlinear variation of the fundamental band gaps *versus* copper concentration. In addition, the phase diagram exhibits the rock salt structure as the ground state for this new ternary system.

References

1. J.F. Hamilton, *Adv. Phys.* **37**, 359 (1988).
2. B.E. Mellander, *Phys. Rev. B* **26**, 5886 (1982).
3. E. Frolich, E. Moler, P. Weiesner, *Phys. Rev. Lett.* **26**, 554 (1971).
4. M. Cardona, *Phys. Rev.* **129**, 69 (1963).
5. M. Ameri, D. Hachemane, I. Ameri, B. Abidri, B. Bouhafis, D. Varshney, Y. Al-Douri, *Can. J. Phys.* **53**, 2 (2015).
6. M. Ameri, N. Bouzouira, M. Doui-Aici, R. Khenata, A. Yakoubi, B. Abidri, N. Moulay, M. Maachou, *Mater. Sci. Appl.* **2**, 749 (2011).
7. B. Amrani, F. El HajHassan, R. Khenata, H. Akbarzadeh, *J. Phys. Chem. Solids* **70**, 1055 (2009).
8. F. Badi, S. Louhibi, M.R. Aced, N. Mehnane, N. Sekkal, *Physica E* **41**, 45 (2008) (with LDA).
9. S. Savrasov, D. Savrasov, *Phys. Rev. B* **46**, 12181 (1992).
10. W. Kohn, L.J. Sham, *Phys. Rev. A* **140**, 1133 (1965).
11. S.Y. Savrasov, *Z. Kristallogr.* **220**, 555 (2005).
12. J.P. Perdew, Y. Wang, *Phys. Rev. A* **45**, 13244 (1992).
13. J.P. Perdew, S. Burke, M. Ernzerhof, *Phys. Rev. Lett.* **77**, 3865 (1996).
14. F.D. Murnaghan, *Proc. Natl. Acad. Sci. U.S.A.* **30**, 5390 (1944).
15. R.W.G. Wyckoff, *Crystal Structures* (Wiley, New York, 1963).
16. S. Hull, D. Keen, *Phys. Rev. B* **50**, 5868 (1994).
17. S. Hull, D.A. Keen, *Phys. Rev. B* **59**, 750 (1998).
18. B. Amrani, T. Benmessabih, M. Tahiri, I. Chihoub, S. Hiadi, F. Hamdache, *Physica B* **381**, 179 (2006) (with GGA).
19. T. Benmessabih, B. Amrani, *Physica B* **392**, 309 (2007).
20. L.A. Palomino-Rojas a, M. Lo ´pez-Fuentes, *Solid State Sci.* **10**, 1228 (2008).
21. S. Hull, D. Keen, *Phys. Rev. B* **50**, 5868 (1994).
22. R.C. Hanson, J.R. Hallberg, C. Schwab, *Appl. Phys. Lett.* **21**, 490 (1972).
23. S. Hull, D.A. Keen, *Phys. Rev. B* **59**, 750 (1998).
24. L. Vegard, *Z. Phys.* **5**, 393 (1921).
25. B. Batlogg, J.P. Remeika, R.G. Maines, *Solid State Commun.* **38**, 83 (1981).
26. D. Westphal, A. Goldman, *J. Phys. C* **15**, 6661 (1982).
27. K.H. Hellwege, O. Madelung (Editors), *Semiconductor Physics of II–VI and I–VII Compounds. Semimagnetic Semiconductors, Landolt-Bornstein, New York Series Group III*, Vol. **17**, (Springer, Berlin, 1987) Pt. b.
28. H.-C. Hsueh, J.R. Maclean, G.Y. Guo, M.-H. Lee, S.J. Clark, G.J. Ackland, J. Crain, *Phys. Rev. B* **51**, 12216 (1995).